What can we learn about compact binaries from the kilonova emission?

Agnieszka Janiuk

Multimessenge astrophysics session
Polish Astronomical Society Congress
Toruń, 13.09.2023

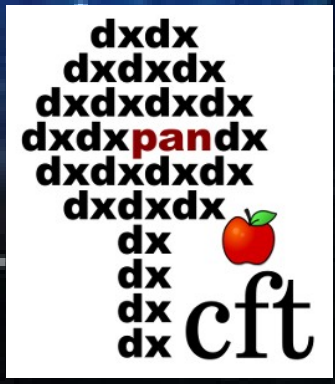

Plan of the talk

1. Introduction, short GRBs, kilonovae, and gravitational waves

2. Postmerger systems

3. Accretion and outflow simulations, and kilonova modeling

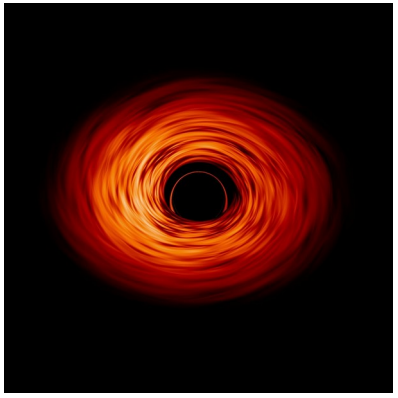

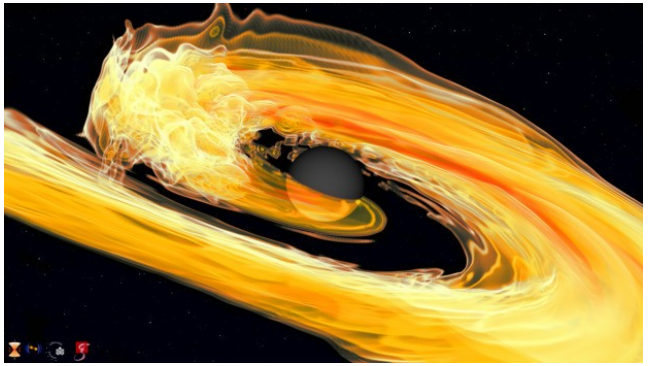

Gamma Ray Bursts

Rapid, bright flashes of radiation peaking in the gamma-ray band

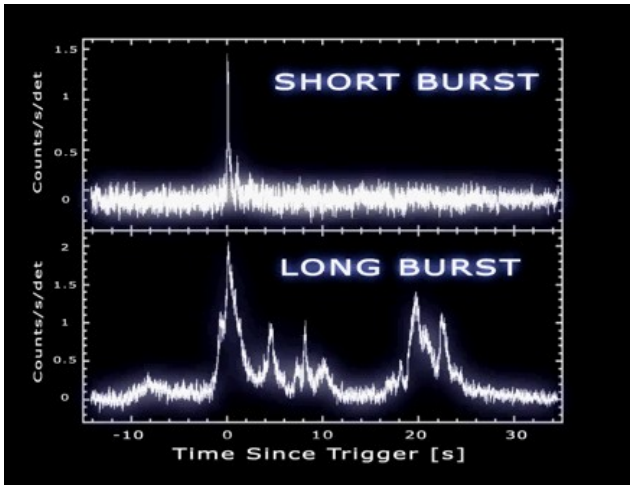

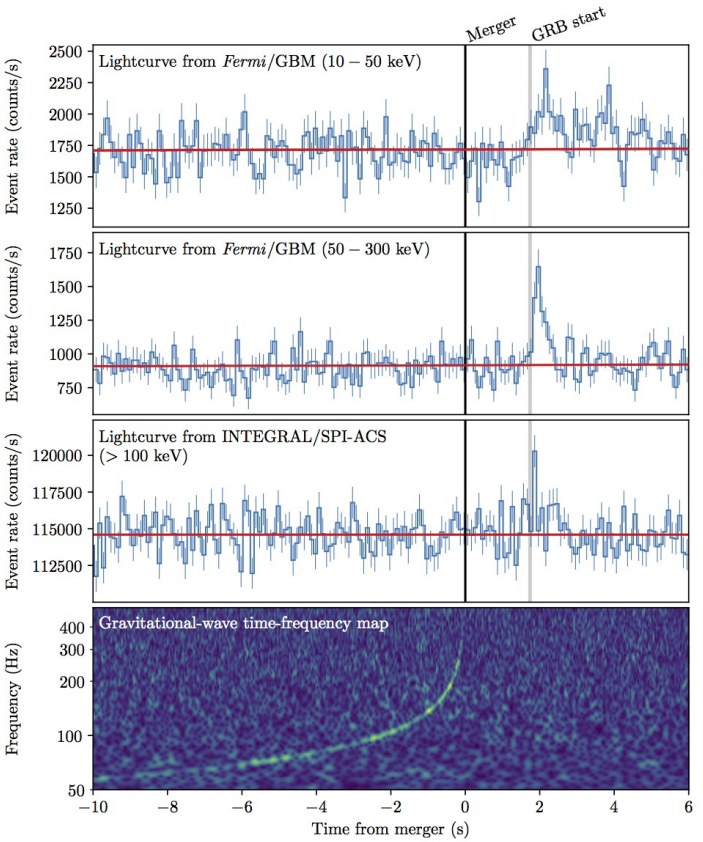

First confirmed progenitor of short GRB: GW170817 (Abbott et al. 2017)

Short GRBs engines: simulations

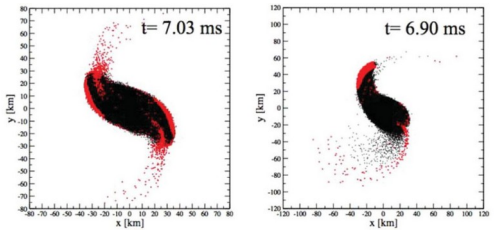

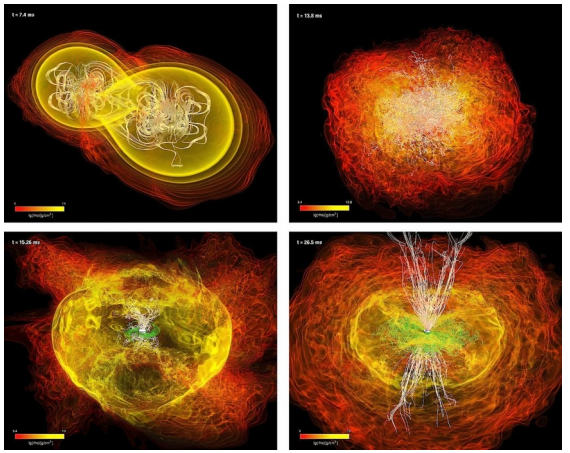

Compact binary mergers

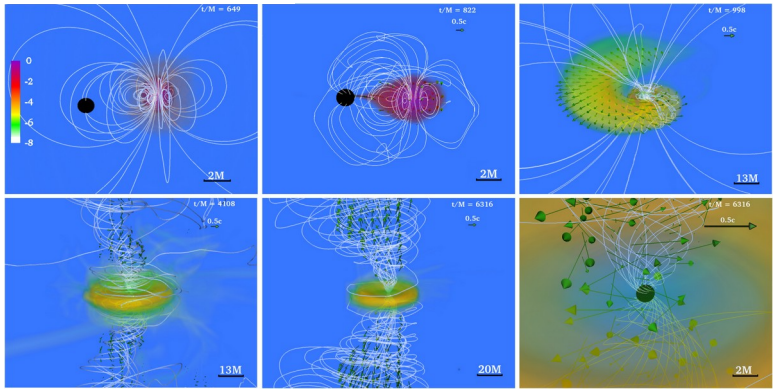

NS-NS and NS-BH (*e.g.Korobkin et al. 2012, Rezzolla et al. 2014, Paschalidis et al. 2015, Shibata, Baumgarte & Shapiro 2000*).

Post-merger systems

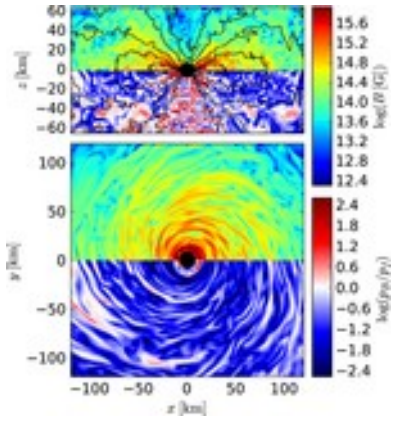

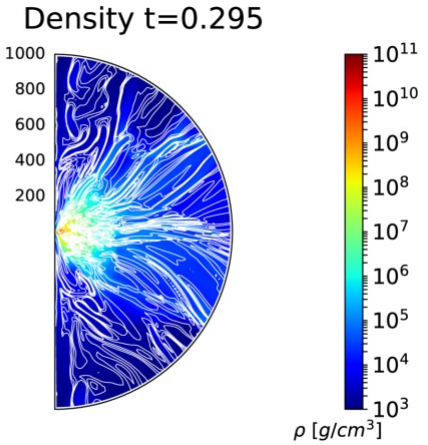

Neutrino-cooled BH accretion disk with nuclear EOS (e.g., Janiuk et al. 2017, 2019; Siegel & Metzger. 2018; Fernandez et al. 2019)

Disk, wind and jet

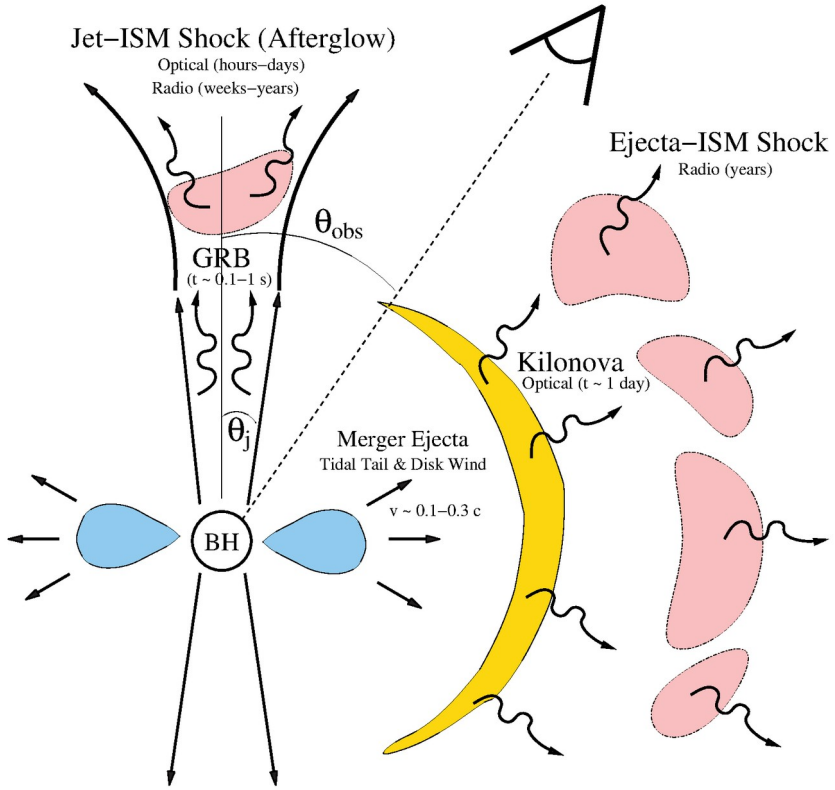

fig. B. Metzger
(Living Reviews in Relativity, 2020).

Potential electromagnetic counterparts of compact object binary mergers as a function of the observer viewing angle.

Rapid accretion of a centrifugally supported disk (blue) powers a collimated relativistic jet, which produces a short GRB.

Equatorial outflows contribute to lower-energy signal.

Both disk wind and jet are powered by the Central Engine –> black hole accretion disk.

Kilonova

NS-NS eject material rich in heavy radioactive isotopes.

Can power an electromagnetic signal called a kilonova

(e.g. Li & Paczynski 1998; Tanvir et al. 2013, Berger 2016)

Dynamical ejecta from compact binary mergers, $M_{ej} \sim 0.01\ M_{Sun}$, can emit about 10^{40}-10^{41} erg/s in a timescale of 1 week

Subsequent accretion can provide bluer emission, if it is not absorbed by precedent ejecta (Tanaka, 2016, Berger 2016, Siegel & Metzger 2017)

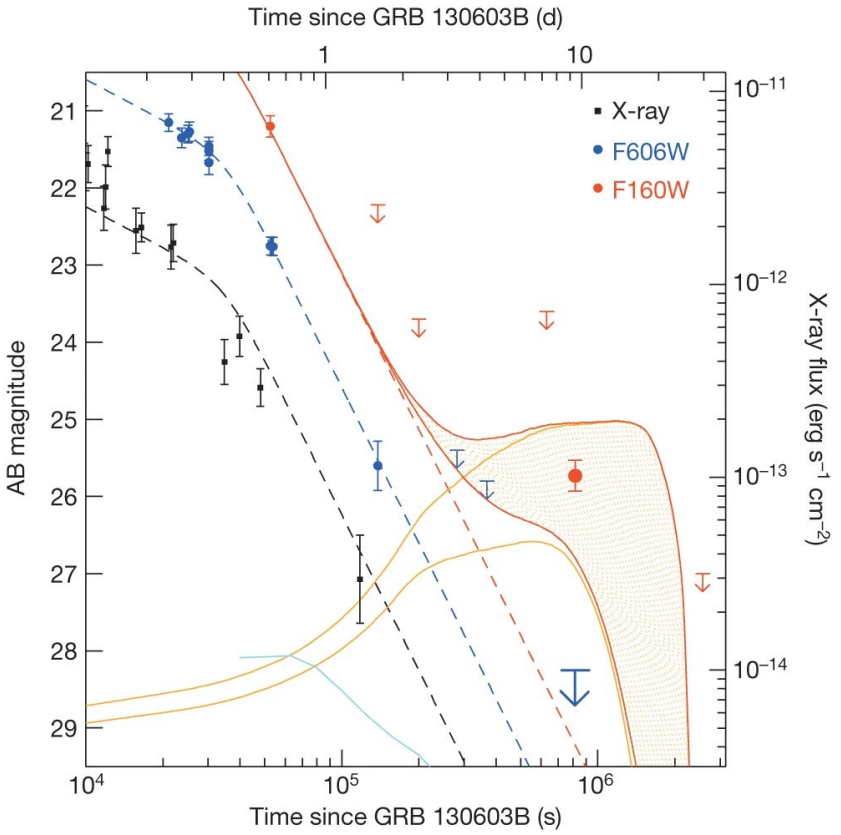

(N. Tanvir et al., 2013, Nature)

GW 170817

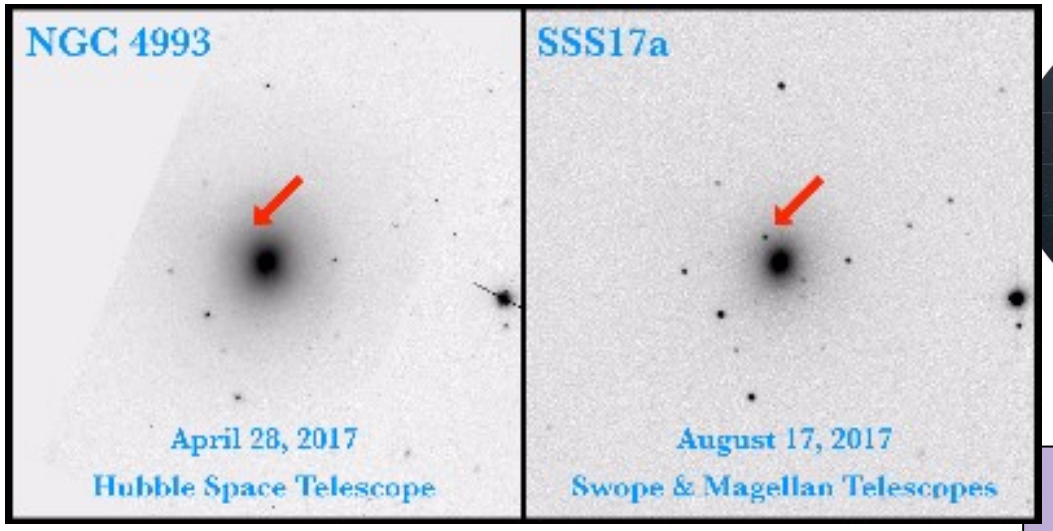

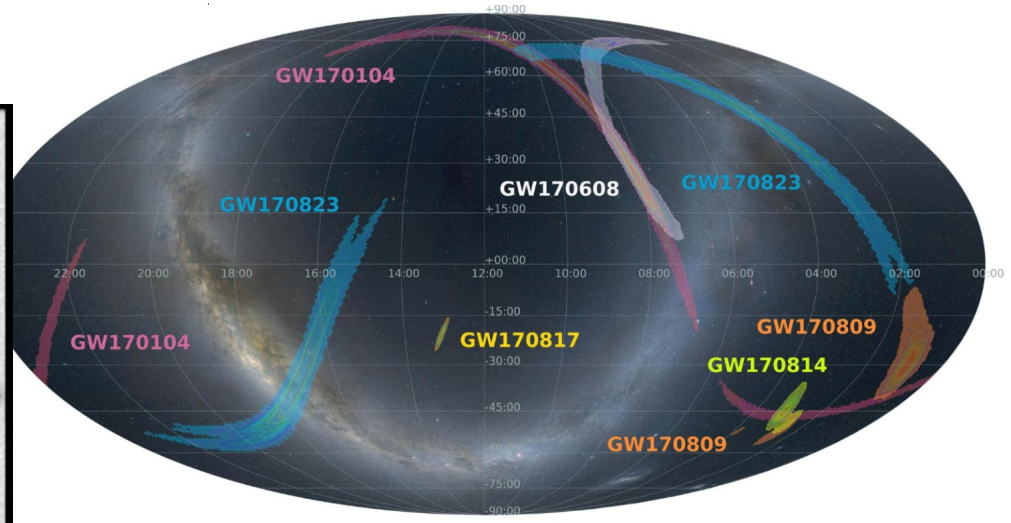

Rapidly fading electromagnetic transient in the galaxy NGC4993, was spatially coincident with GW170817 and a weak short gamma-ray burst (e.g., Smartt et al. 2017; Zhang et al. 2017, Coulter et al. 2017)

Double neutron stars formed a black hole after their merger.

During the inspiral phase, **gravitational waves** were produced.

After the merger, gamma-ray telescopes observed a **burst** of energy.

The time delay of 1.7 s may be associated with formation of HMNS

Blue and red kilonova lightcurves

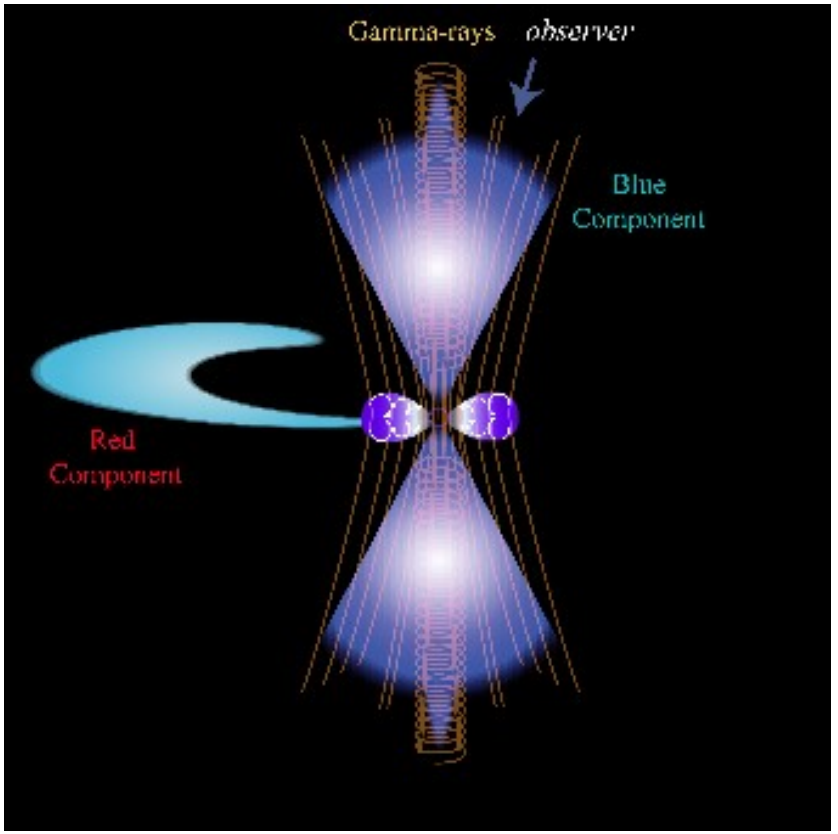

Schematic idea of the GW170817 system in the post-merger phase (Murguia-Berthier et al. 2017).

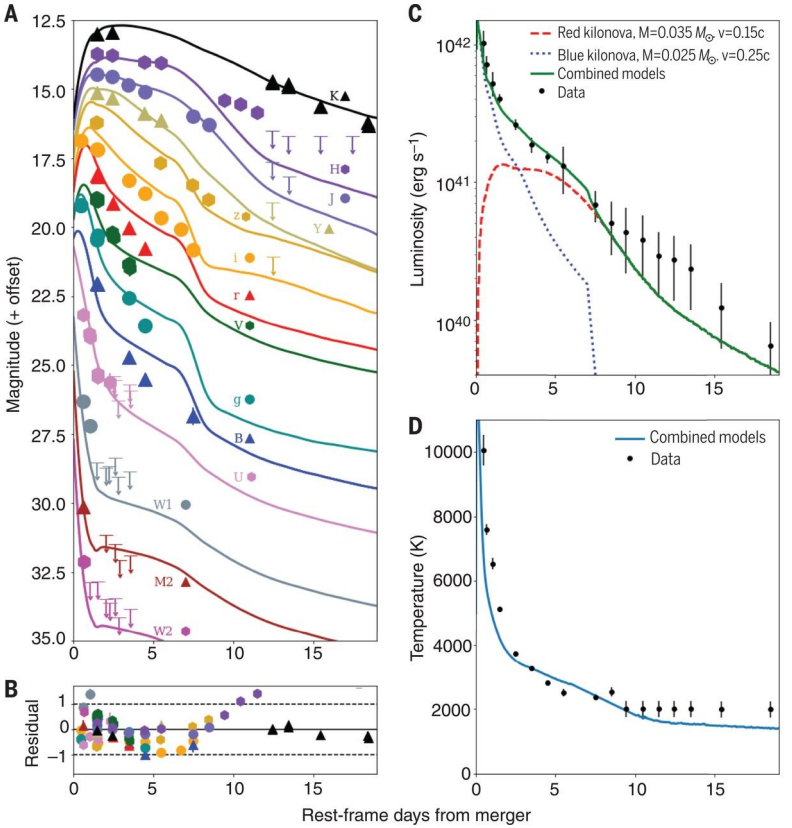

Blue and the red light from a kilonova, compared to observational data for the transient SSS17a, associated with GW170817 (Kilpatrick et al. 2017).

Kilonova colors

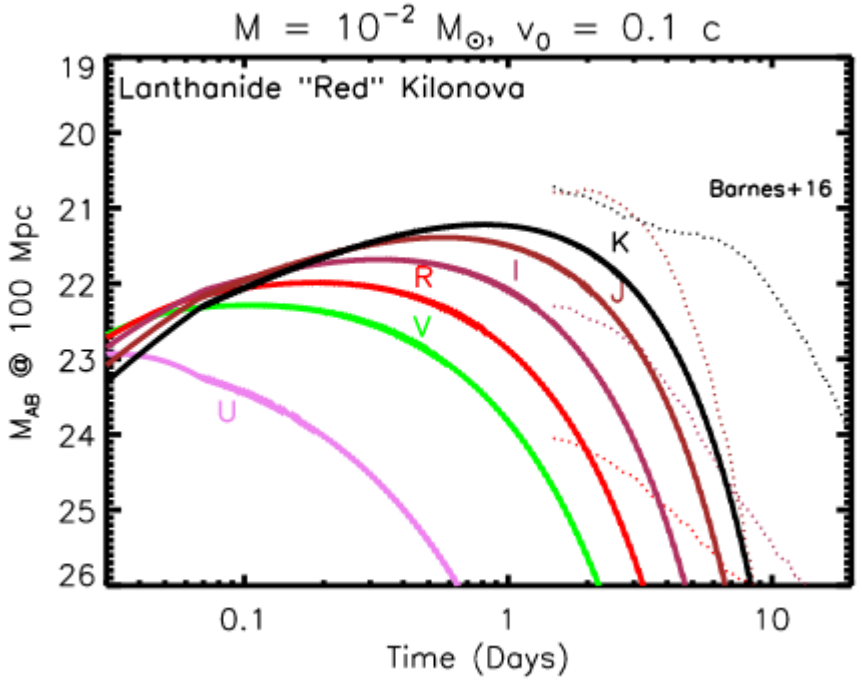

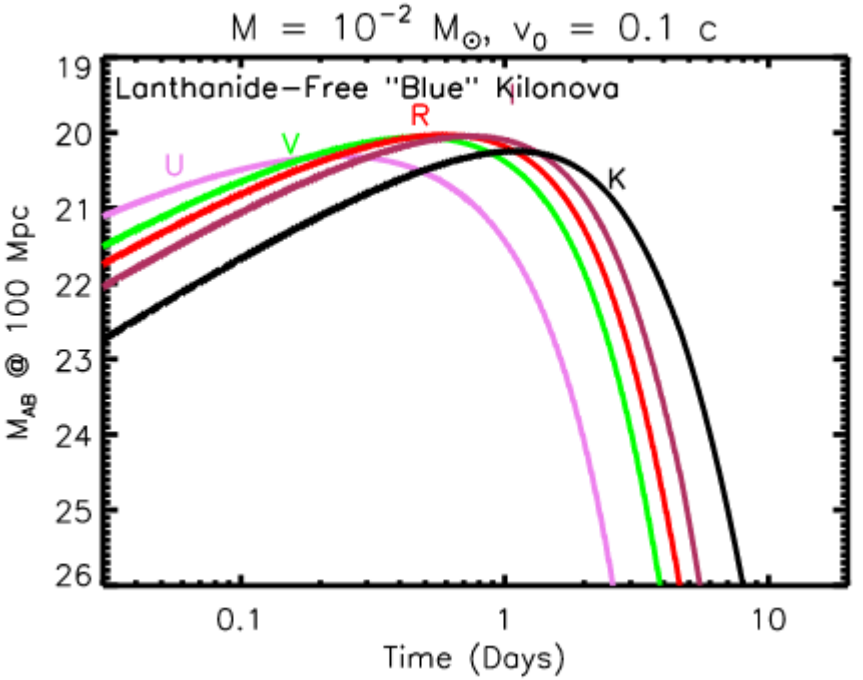

r-process nucleosynthesis

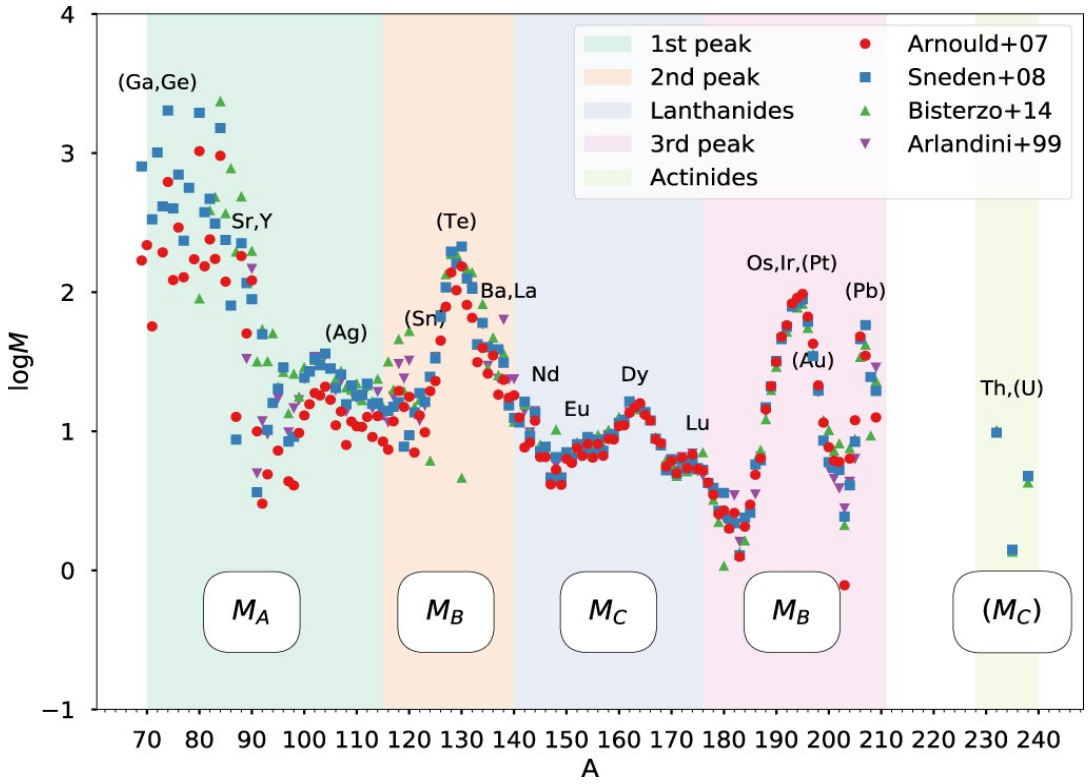

Ji et al. 2019

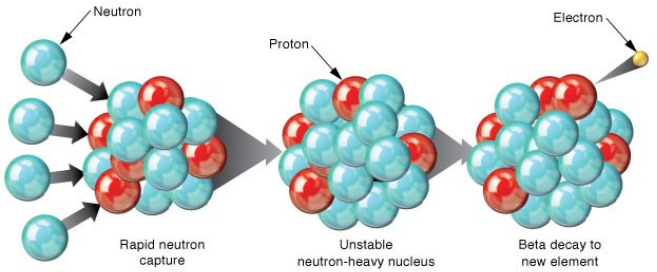

$Y_e > 0.25$: 1st peak

$Y_e = 0.15$-0.25: 2nd peak, Lanthanides

$Y_e < 0.15$: 3rd peak, Actinides

Matter is neutronized, $Y_e = n_p/(n_p + n_n) < 0.5$.

Our GR MHD simulations of central engine

$$T_{(m)}^{\mu\nu} = \rho\xi u^\mu u^\nu + p g^{\mu\nu}$$

$$T_{(em)}^{\mu\nu} = b^\kappa b_\kappa u^\mu u^\nu + \frac{1}{2} b^\kappa b_\kappa g^{\mu\nu} - b^\mu b^\nu$$

$$T^{\mu\nu} = T_{(m)}^{\mu\nu} + T_{(em)}^{\mu\nu},$$

$$(\rho u_\mu)_{;\nu} = 0$$

$$T^\mu_{\nu;\mu} = 0.$$

HARM= High Accuracy Relativistic MHD
Equation of State of ideal gas with analytic form was used in original code (Gammie et al. 2003).

Fermi gas EOS is computed numerically and tabulated during simulation with
P(ρ, T), e(ρ,T) implemented in
(Janiuk et al. 2017, ApJ; Janiuk 2019, ApJ).

Publicly available code version

https://github.com/agnieszkajaniuk/HARM_COOL

- Hyperaccretion: rates of 0.01-a few M_S/s. Nuclear temperatures and densities
- Plasma composed of free n, p, e+, e− pairs, and He nuclei
- Nuclear reactions: electron-positron capture on nucleons, and neutron decay (Reddy, Prakash & Lattimer 1998)
- Neutrino absorption & scattering: two-stream approximation (Di Matteo et al. 2002)

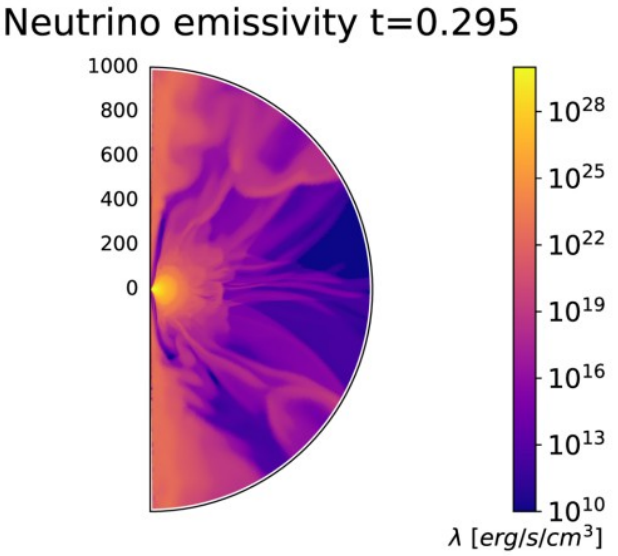

Outflow disk wind

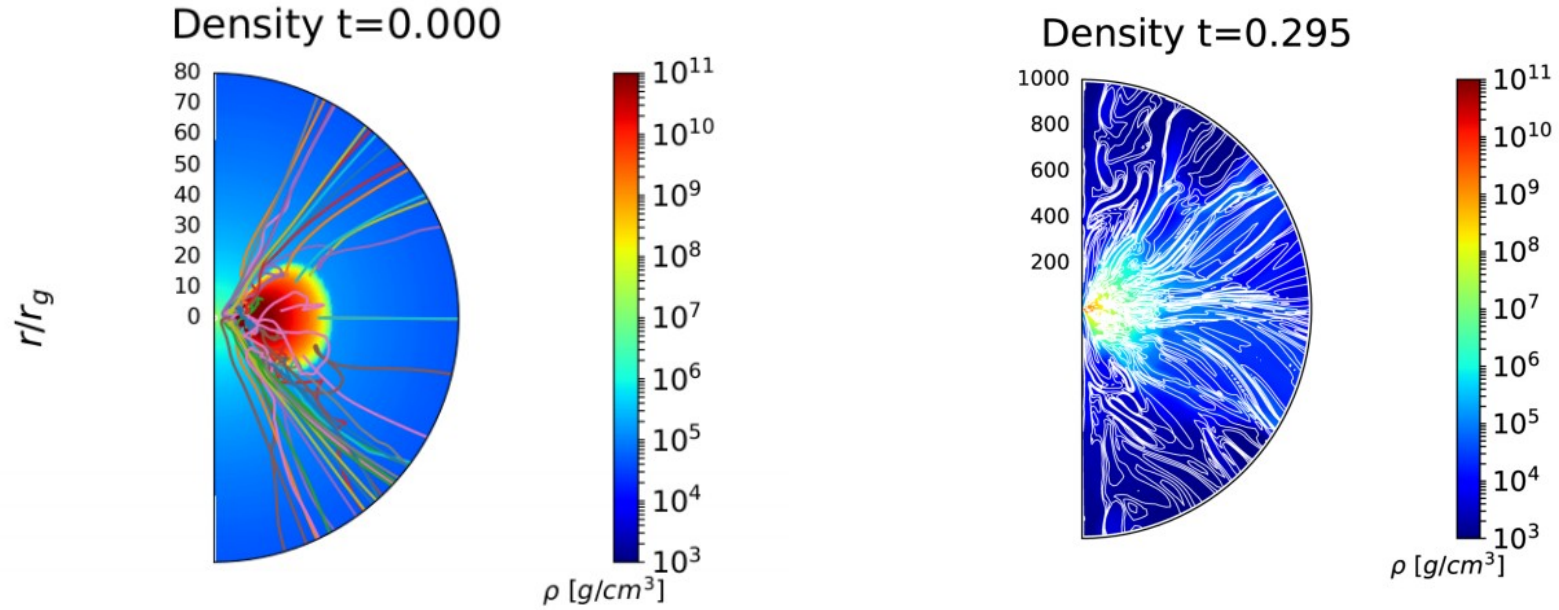

Code **HARM-COOL** (Janiuk, 2019, ApJ, 882, 163)
follows the wind outflow, using tracer particle technique
(Wu et al. 2016; Bovard & Rezzola 2017).

Tracers are Lagrangian particles, which store data about density, velocity, and electron fraction in the outflow.

(see talk by Gerardo Urritia, later today)

Nucleosynthesis in disk wind

Heavy elements up to A ~ 200
(incl. Platinum, Gold) are produced
in disk ejecta.

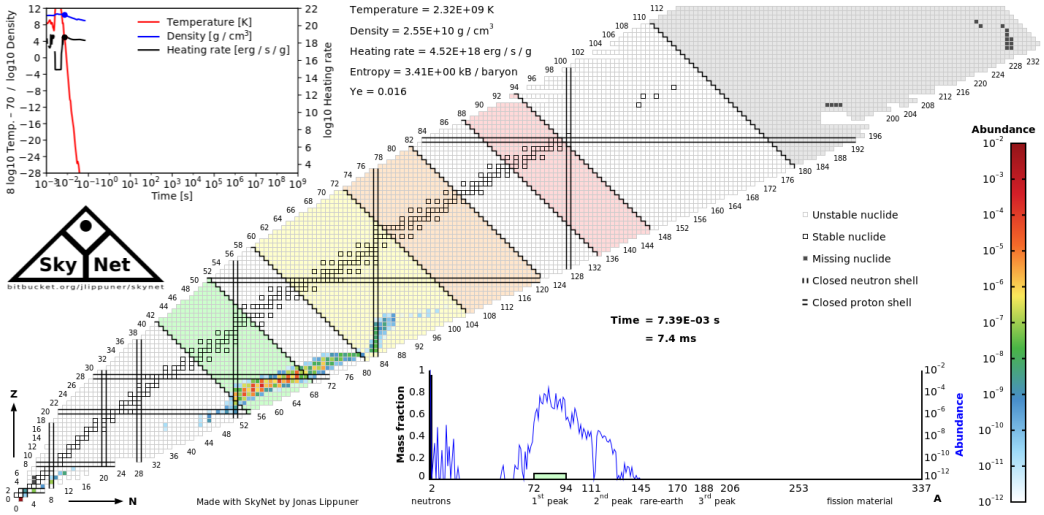

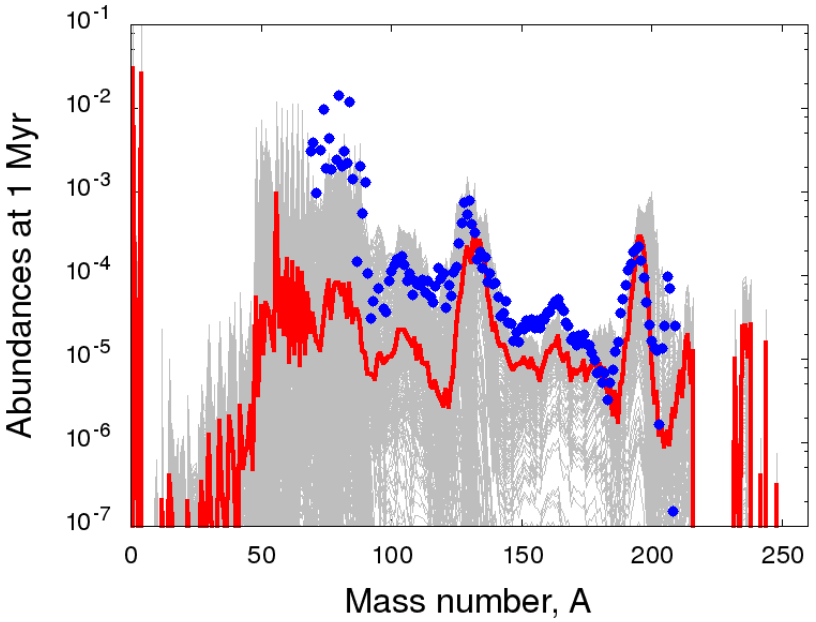

Nucleosynthesis in disk wind
(Janiuk, 2019)

Code **SkyNet**, provides a nuclear reaction network; Lippuner & Roberts (2017).
Publicly available, with a user-friendly python interface.

r-process nucleosynthesis is calculated by postprocessing of tracer data, to obtain chemical evolution of the wind

Disk wind properties

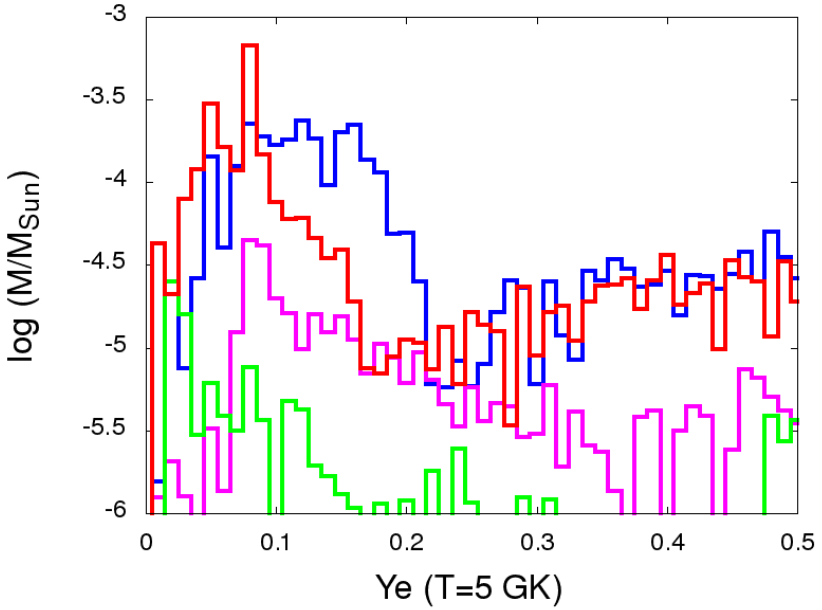

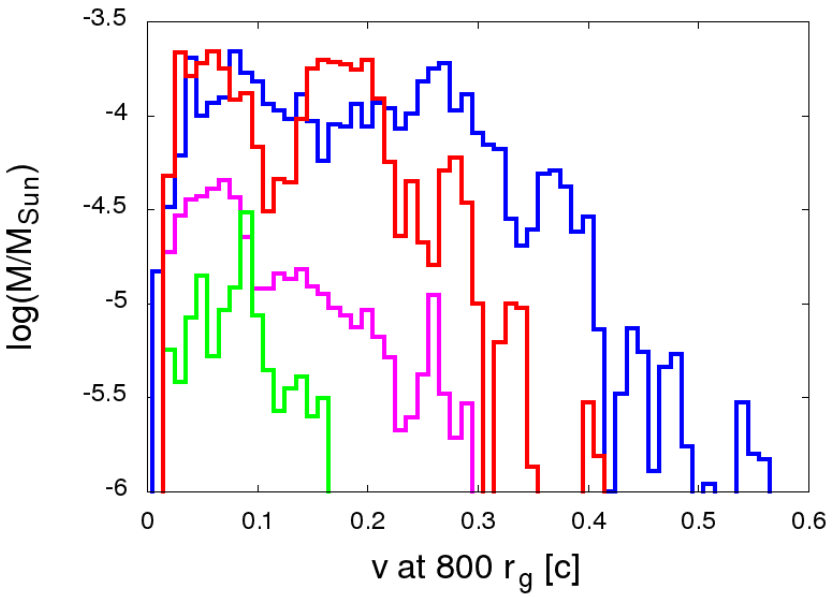

The disk launch fast wind outflows (v=c ∼ 0.11 − 0.23) with a broad range of electron fraction Ye ∼ 0.1 − 0.4. Mass loss via unbound outflows is between 2% and 17% of the initial disk mass. **The outflow composition is sensitive to engine parameters: BH spin and magnetisation of the disk**

More magnetized disk produce faster outflows. Smaller BH spins produce more fraction of neutron rich ejecta

Populations of kilonova progenitors

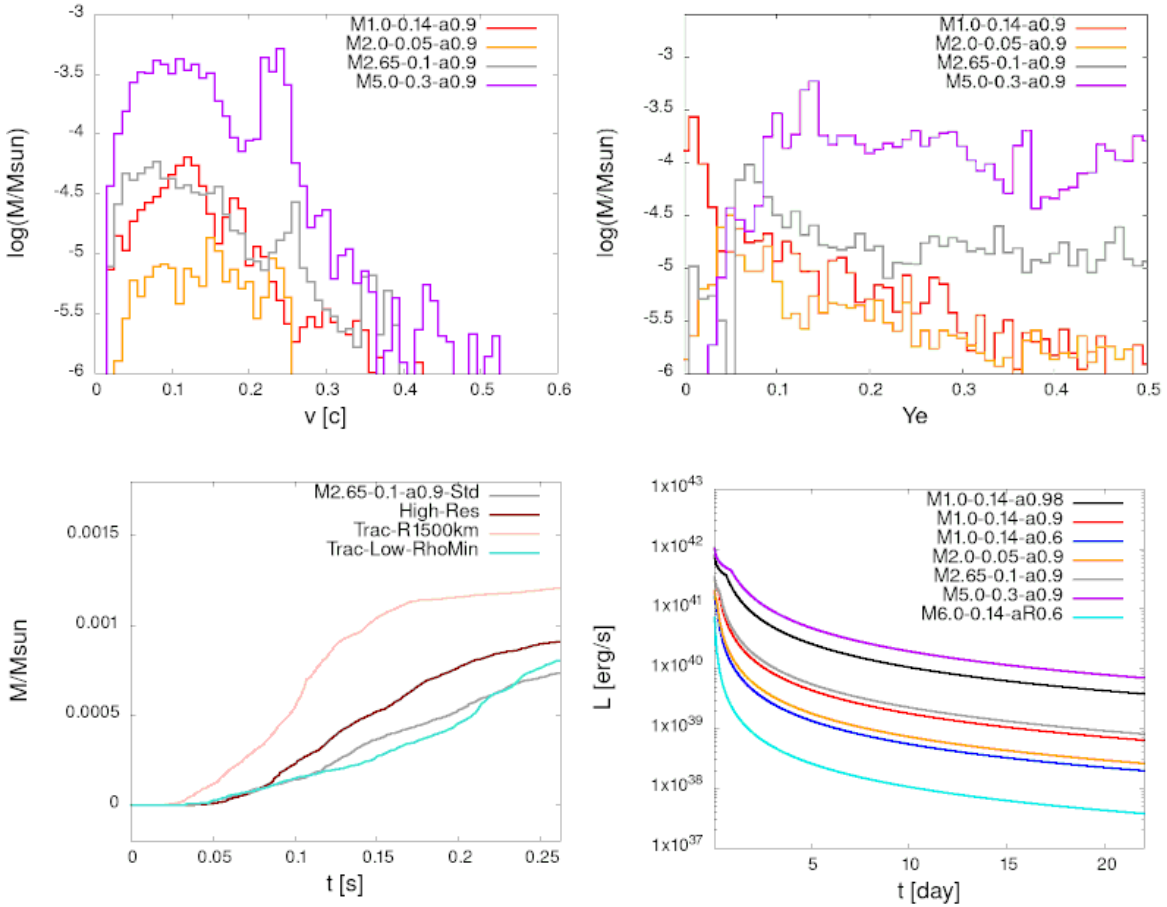

F. H. Nouri, A. Janiuk & M. Przerwa (2023, ApJ, 944, 220)

We find strong correlation between the black hole's spin and ejected mass.

Drozda et al. (2022) found that only a fraction (∼20%) of BHNS binaries gain a high BH spin.

Synthetic kilonova lightcurves

We calculated synthetic kilonova ligtcurves for a range of BH-disk mass ratios and range of black hole spin parameters.

Our models do not provide direct method to distinguish between BH-NS and NS-NS progenitors, but the LC slopes my me affected by progenitor type (Kasen et al. 2015).

Creation of a magnetized and differentially rotating HMNS with different lifetimes can also affect the amount of ejected matter, hence LC slope (de Haas et al. 2022).

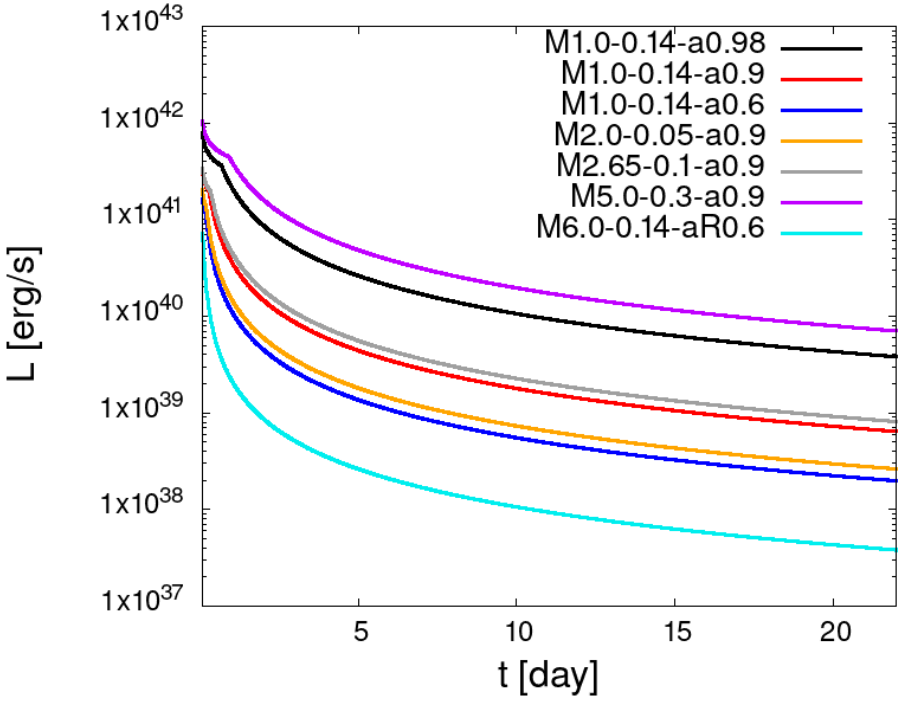

Kilonova with long GRB

On 11 December 2021, the Fermi GBM triggered and located GRB 211211A which was also detected by the Swift/BAT (D'Ai et al., GCN 31202).

The GBM light curve consists of an exceptionally bright emission made up of three separate pulses with a duration (T90) of about 34.3s (50-300 keV) (Mangan et al., GCN 31210).

GRB 211211A: hybrid event, analogous to GRB 060614.

hard spectrum, short variability timescale and negligible temporal lag.

not locate in any star-forming region and associacion with supernova is excluded (Troja et al. 2022, Nature).

A kilonova component is identified in the UV/optical/infrared by spectral analysis (Rastinejad et al., 2022, Nature)

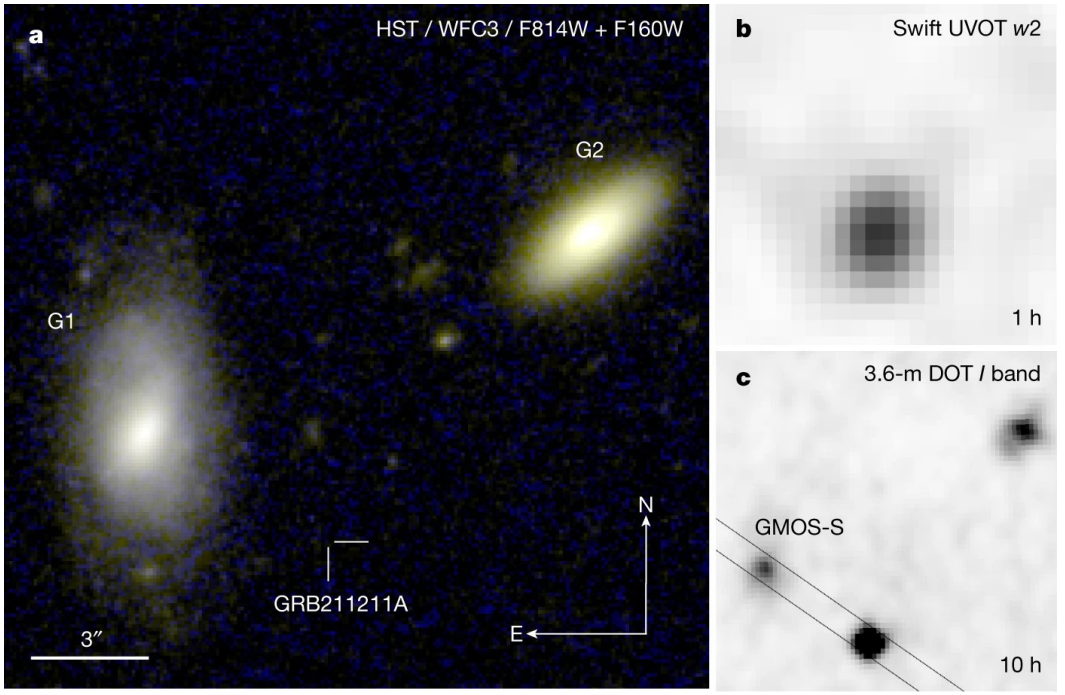

GRB 211211A

Neutrino lightcurves

The neutrino leakage scheme employed following
Ott et al. (2021)
https://stellarcollapse.org
is implemented in **HARM-COOL-NUC**

Three-parameter EOS: $\epsilon(\rho, T, Y_e)$, $P(\rho, T, Y_e)$.

A. Janiuk, 2023,
ArXiV:2303.18129

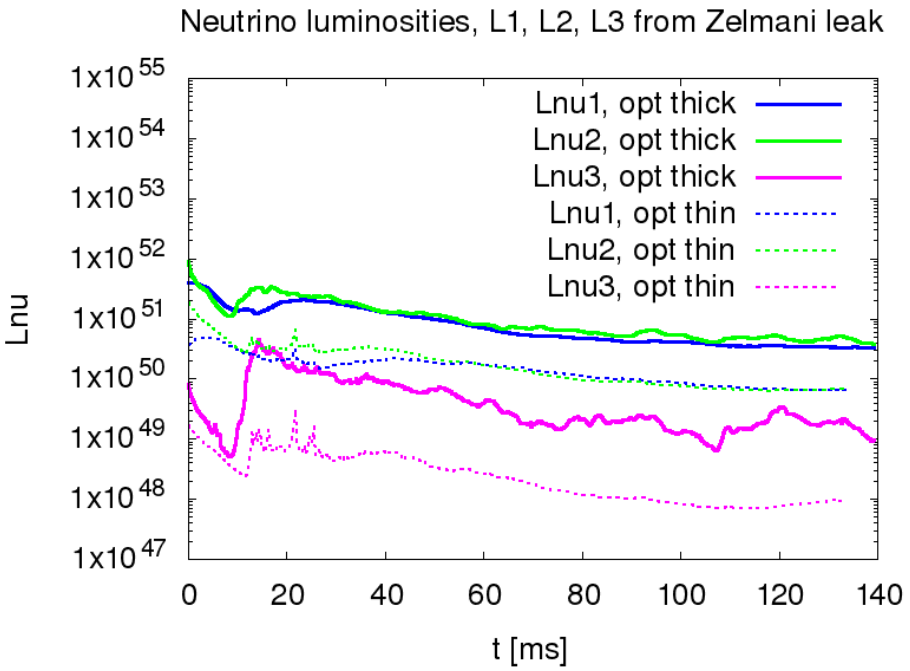

L1- electron neutrino
L2- electron antineutrino
L3 - other favors (nux)

Neutrino spectra

These neutrinos can be potentially detectable by upcoming MeV neutrino detectors.

The neutrino ‘horizon’ is estimated at ∼0.61–0.77 Mpc, 0.10 Mpc, and 0.18 Mpc for Hyper-K, JUNO and LENA, respectively (Liu et al. 2015)

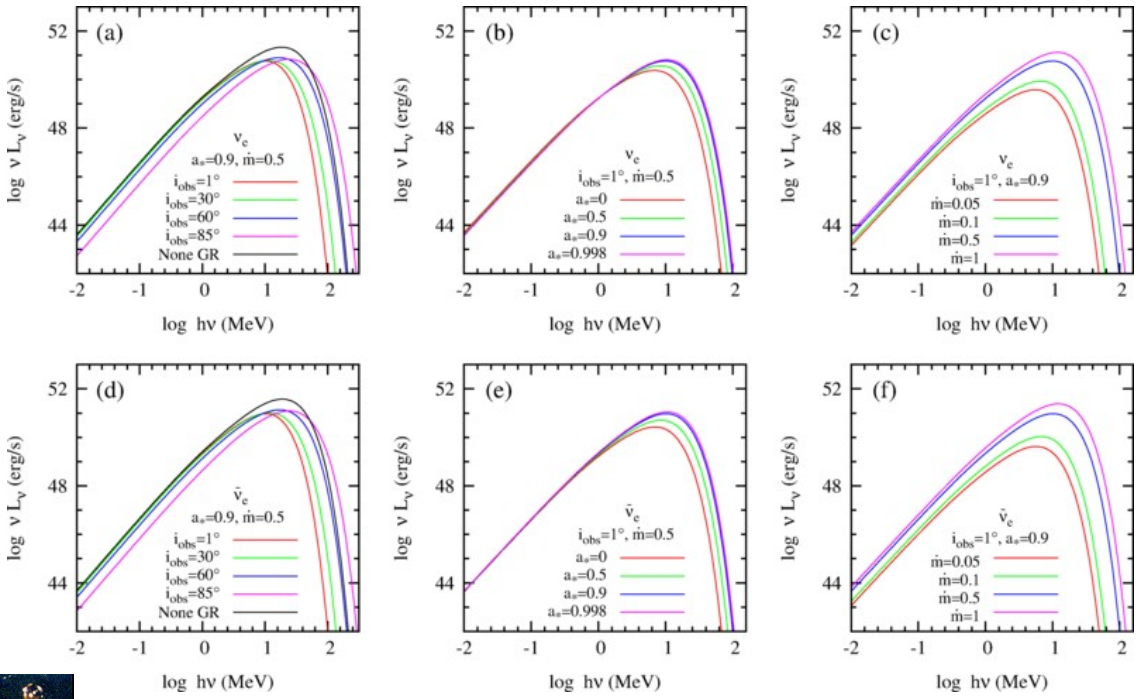

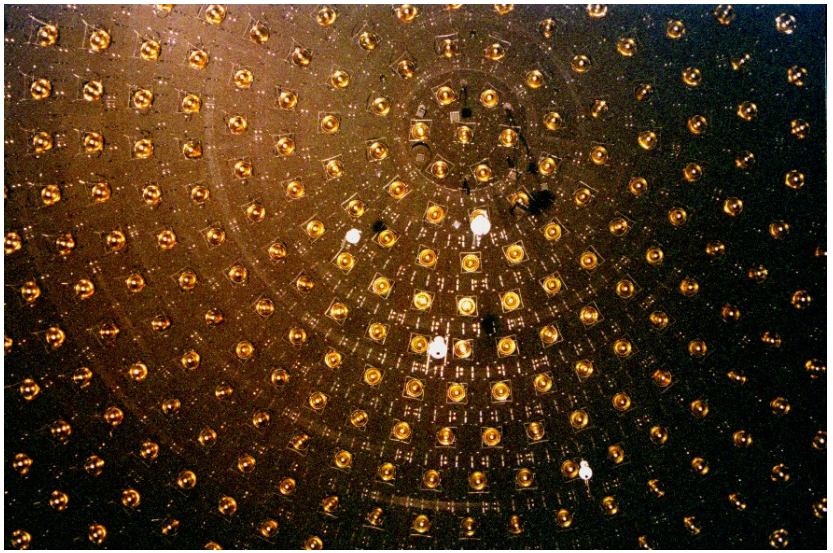

Spectra from 1-D stationary, simplified NDAF model (Liu et al. 2015)

Relativistic Astrophysics group at CTP PAS

- please visit our website.

https://ra.cft.edu.pl/

Accretion disk's environmental effects on gravitational waves from LISA for extreme mass ratio black hole binaries

Fatemeh Hossein Nouri and Agnieszka Janiuk
Center for Theoretical Physics, Polish Academy of Sciences, Al. Lotnikow 32/46, 02-668 Warsaw, Poland

The merger of supermassive black holes (BBH) produces mHz gravitational waves (GW), which are potentially detectable by future Laser Interferometer Space Antenna (LISA). Such binary systems are usually embedded in an accretion disk environment at the centre of the active galactic nuclei (AGN). Recent studies suggest the plasma environment imposes measurable imprints on the GW signal if the mass ratio of the binary is around $q \sim 10^{-4} - 10^{-3}$. The effect of the gaseous environment on the GW signal is strongly dependent on the disk's parameters, therefore it is believed that future low-frequency GW detections will provide us with precious information about the physics of AGN accretion disks. We investigate this effect by measuring the disk torques on the binary system by modelling several magnetized tori. Using GRMHD HARM-COOL code, we perform 2D simulations of weakly-magnetized thin accretion disks, with a possible truncation and transition to advection-dominated accretion flow (ADAF). In our numerical simulations, we study the angular momentum transport and turbulence generated by the magnetorotational instability (MRI). We quantify the disk's effective alpha viscosity and its evolution over time. We apply our numerical results to estimate the relativistic viscous torque and GW phase shift due to the gas environment.

- new paper today
ArXiV:2309.06028

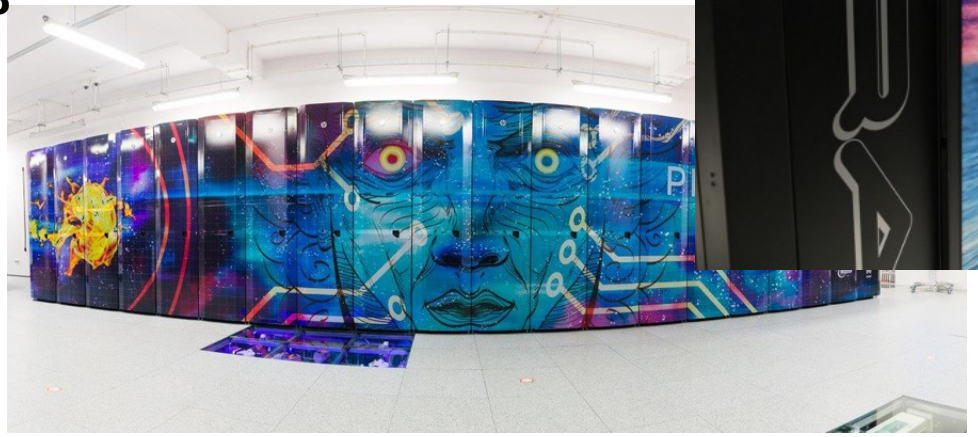

dxdx
dxdxdx
dxdxdxdx
dxdxpandx
dxdxdxdx
dxdxdx
dx
dx
dx
dx cft

PL GRID

NARODOWE CENTRUM NAUKI

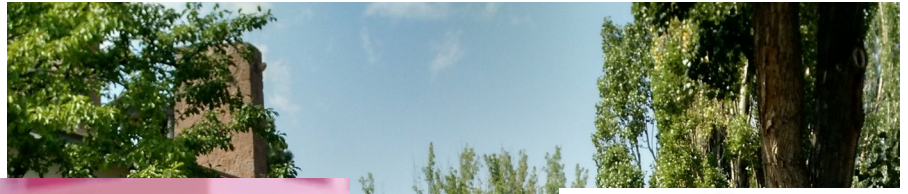


Ken

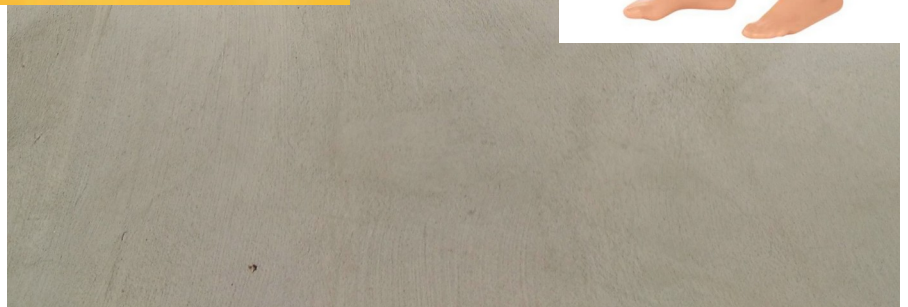

The key conclusion from this plot is that the source seen in the NIR requires an additional component above the extrapolation of the afterglow (red dashed line), assuming that it also decays at the same rate. This excess NIR flux corresponds to a source with absolute magnitude $M(J)AB \approx -15.35$ mag at ~ 7 d after the burst in the rest frame. This is consistent with the favoured range of kilonova behaviour from recent calculations (despite their known significant uncertainties), as illustrated by the model lines (orange curves correspond to ejected masses of 10^{-2} solar masses (lower curve) and 10^{-1} solar masses (upper curve), and these are added to the afterglow decay curves to produce predictions for the total NIR emission, shown as solid red curves). The cyan curve shows that even the brightest predicted r-process kilonova optical emission is negligible.

a) False colour image combining optical (F814W; blue) and near-infrared (F160W; red and green) HST observations of GRB 211211A, carried out with the Wide Field Camera 3 (WFC3) camera in April 2022 (approximately 4 months after the burst). Two bright galaxies (G1 at $z \approx 0.0762$, and G2 at $z \approx 0.4587$) and several fainter ones are visible, but no source is detected at the location of GRB 211211A. The most probable host galaxy is G1, a low-mass, late-type galaxy. The projected physical offset between the burst and the centre of the galaxy is approximately 8 kpc, one of the largest ever measured for a long burst. b,c, The same field is shown in the UV w2 filter observed by Swift at 1 h after the burst (b), and in the optical I filter acquired by the 3.6-m DOT/4K × 4K CCD imager at 10 h after the burst (c). The solid lines show the slit position used for optical spectroscopy with Gemini/GMOS-S. The bright UV counterpart rules out a high-redshift origin, whereas its rapid reddening is consistent with the onset of a kilonova.

2D simulation results of neutrino-thin and thick disks

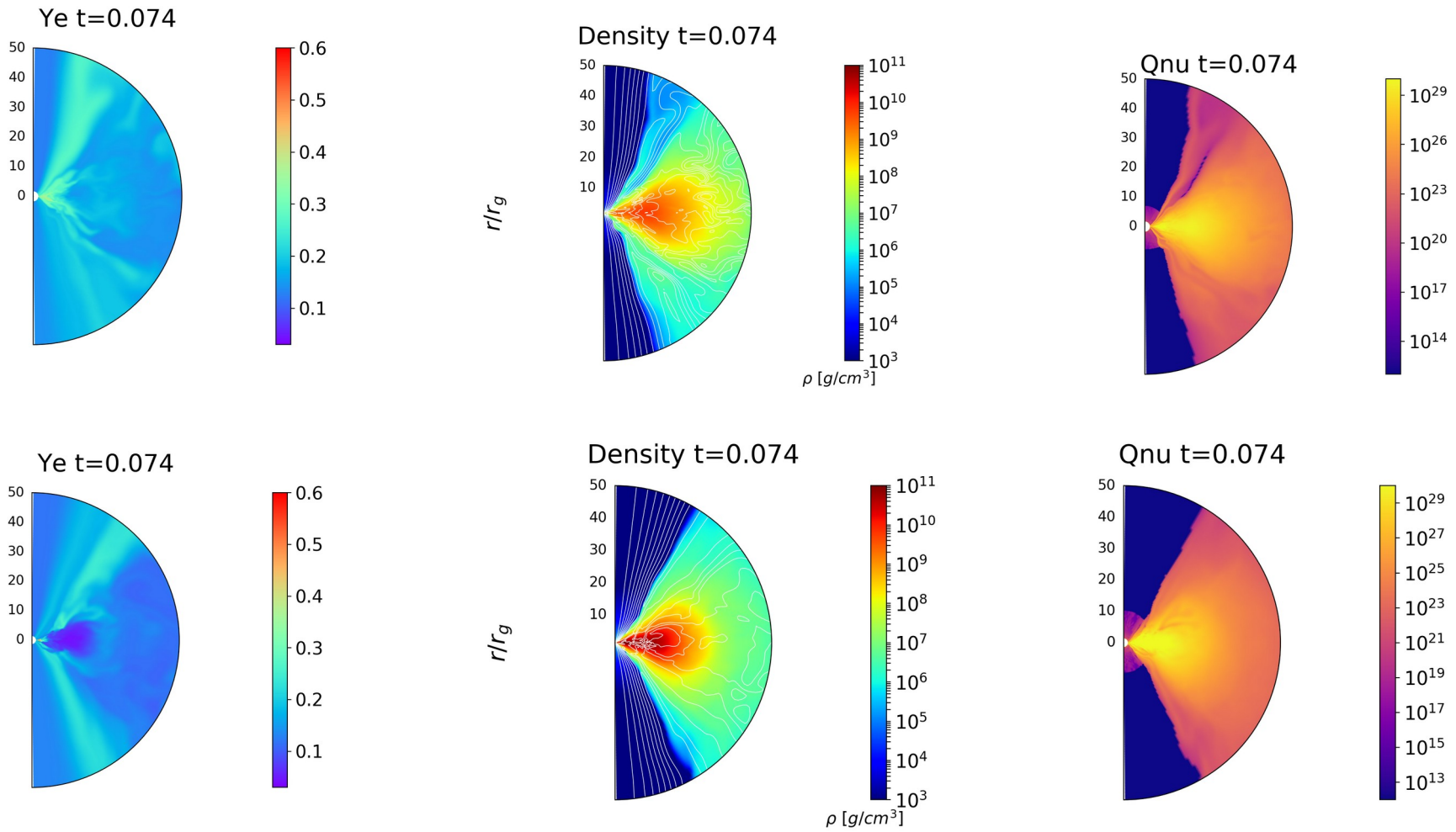

Current HARM-COOL-Nu scheme:

Additional source term iin the energy-momentum conservation equation, due to heating and cooling by neutrinos. Net rate of neutrino emission computed from lepton number conservation

GR MHD with Composition dependent EOS

$$\partial_t \mathbf{U(P)} = -\partial_i \mathbf{F^i (P)} + \mathbf{S(P)}$$

Non-trivial transformation between ‘conserved’ and ’primitives’ variables in GR MHD.

- Various inversion schemes tested (cf. Siegel 2019).
- Finally, we used bracketed root-finding method of Palenzuela et al. (2015).

Three-parameter EOS: $\epsilon(\rho, T, Y_e)$, $P(\rho, T, Y_e)$.

In the new code version, we use the Equation of State adapted from **Helmholtz tables**, for wider range of densities and temperatures. We also employ neutrino leakage (Ott et al. 2021)

Preliminary results: A. Janiuk, 2023, **ArXiV:2303.18129**

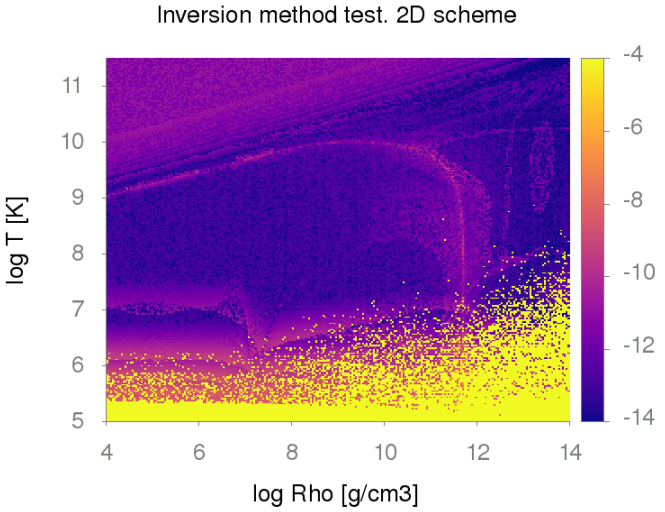

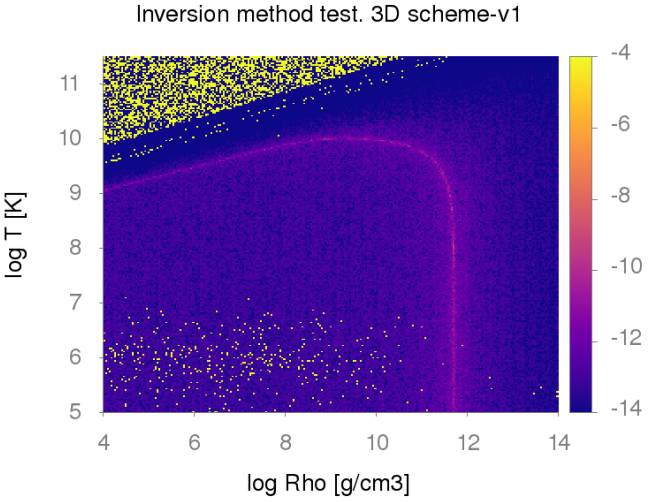

Conserved variables

Explicit form of primitive and conserved variables, fluxes, and source terms, is:

$$\mathbf{P} = [\rho,\ \mathcal{B}^k,\ \tilde{u}^i,\ Y_e,\ T]$$

$$\mathbf{U}(\mathbf{P}) = \sqrt{-g}[\rho u^t,\ T^t_t + \rho u^t,\ T^t_j,\ B^k,\ \rho Y_e u^t]$$

$$\mathbf{F}^i(\mathbf{P}) = \sqrt{-g}[\rho u^i,\ T^i_t + \rho u^i,\ T^i_j,\ (b^i u^k - b^k u^i),\ \rho Y_e u^i]$$

$$\mathbf{S}(\mathbf{P}) = \sqrt{-g}[0,\ T^\kappa_\lambda \Gamma^\lambda_{t\kappa} + \mathcal{Q} u_t,\ T^\kappa_\lambda \Gamma^\lambda_{t\kappa} + \mathcal{Q} u_i,\ 0,\ \mathcal{R}]$$

Here $B^i = \mathcal{B}^i/\alpha = {}^*F^{it}$ is magnetic field, and $\tilde{u}^\mu = (\delta^\mu_\nu + n^\mu n_\nu)u^\nu$ is the projected four-velocity, where the orthognal frame velocity is $n_\mu = [-\alpha, 0, 0, 0]$, $n^\mu = [1/\alpha, -\beta^i/\alpha]$, with lapse $\alpha = 1/\sqrt{g^{tt}}$, and shift function $\beta^i = -g^{ti}/g^{tt}$.
The fluid three velocity is then $v^i = \tilde{u}^i/\gamma = \tilde{u}^i/\alpha u^t$.

Emission simulations

- Day-timescale emission comes at optical wavelengths from lanthanide-free components of the ejecta, and is followed by week-long emission with a spectral peak in the near-infrared (NIR).

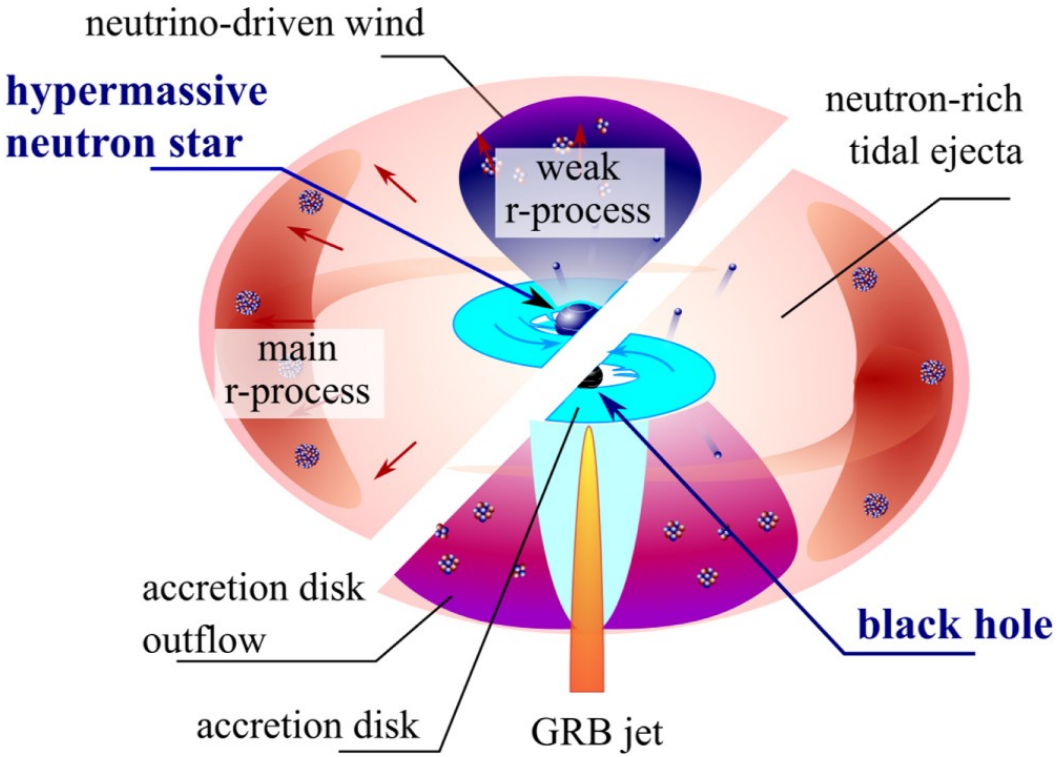

Two-component model scheme (Korobkin et al. 2021)

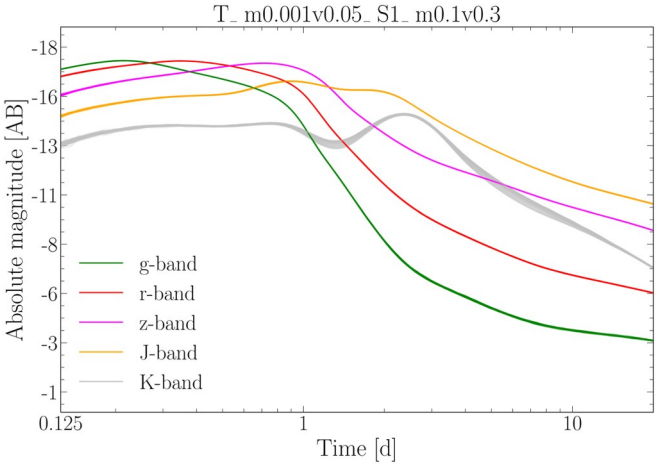

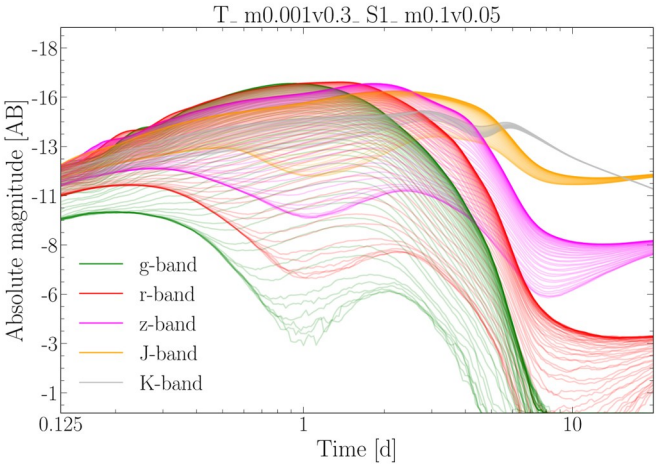

Monte Carlo radiative transfer software SuperNu (Wollaeger & van Rossum 2014) . Two models with 0.001 M⊙ and 0.1 M⊙ in the low-Ye and high-Ye component, respectively. Top: low-Ye and high-Ye ejecta speed of 0.05 c and 0.3 c, respectively. Bottom: low-Ye and high-Ye ejecta speed of 0.3 c and 0.05 c, respectively.

Jet interactions with pre- and post-merger ejecta

In BNS merger, the interaction of a relativistic jet with the ejecta shapes the structure of outflow and its radiation properties.

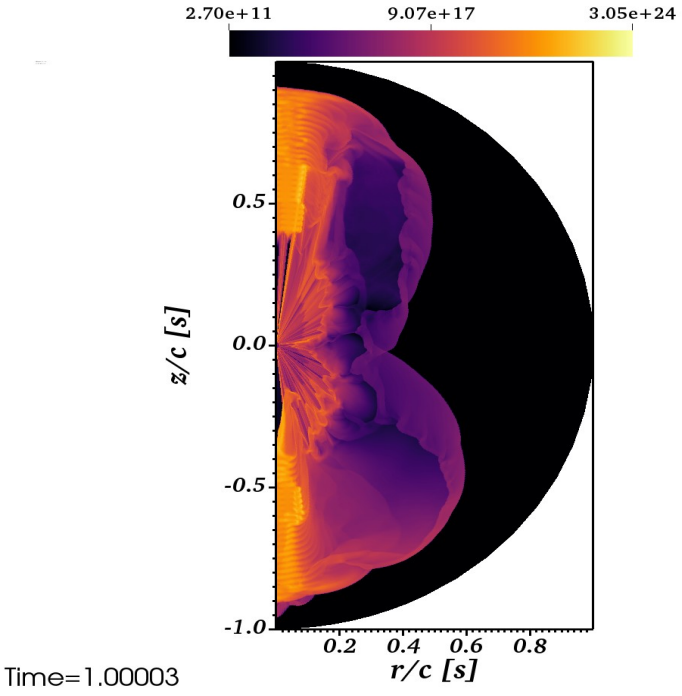

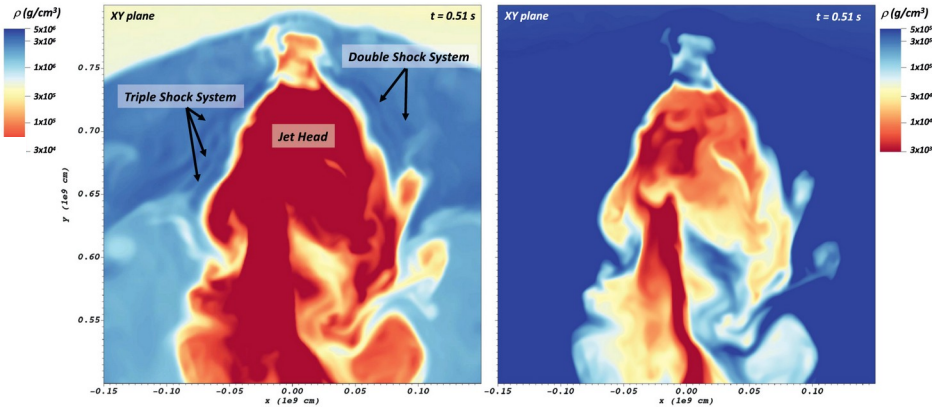

3D simulations show that jet centroid oscillates around the axis of the system, due to inhomogeneities encountered in the propagation (Lazzati et al., 2021)

The breakout time is comparable to the central engine duration and possibly a non-negligible fraction of the total delay between the gravitational and gamma-ray signals. We study this with larger scale, AMR-based simulations. (Urrutia, Janiuk, et al., 2023, in prep.)